Data-partitioned Video Streaming Scheme for Broadband WiMAX

Laith Al-Jobouri, Martin Fleury, Salah M. Saleh Al-Majeed and Mohammed Ghanbari
School of Computer Science and Electronic Engineering
University of Essex, Colchester, United Kingdom
lamoha, fleum, ssaleha, ghan}@essex.ac.uk

***Abstract*—Data partitioning is a way of separating out data from a compressed bitstream according to its importance in reconstructing a video stream. This paper notices that this procedure also results in relatively smaller packets for more important data if the quantization parameter (QP) is set accordingly. Raptor channel coding is then applied and the quality of the video is improved by distributing a significant proportion of intra-coded macroblocks within predictively coded frames. When this scheme is applied to an IEEE 802.16e (mobile WiMAX) system, according to frame size a number of trade-offs arise in respect to balancing the number of packet drops, corrupted packets through channel conditions, overall video quality, and data latency.**

Keywords-broadband wireless, data-partioning, rateless channel coding, source coding, video streaming

I. INTRODUCTION

The features of state-of-the-art codecs can be exploited for video streaming over broadband wireless access IEEE 802.16e (mobile WiMAX) [1], just as for ADSL access networks the higher compression ratios achievable with these codecs can reduce bandwidth demand [2]. The H.264/Advanced Video Coding (AVC) codec, as part of its network-friendly approach, introduces Network Abstraction Layer units (NALUs) as a per-slice container for transmission. While research has investigated NALU packetization issues over wireless networks such as segmentation and aggregation [3], data partitioning of NALUs into A-, B-, and C-partition types [4] of decreasing importance for decoder reconstruction purposes deserves attention as an alternative packetization strategy. This is because when the quantization parameter is set appropriately the size of the A- and B-partitions becomes much smaller than the C-partition. Thus, A- and B-partition NALUs are less at risk from channel error. Video quality in the scheme is additionally improved through the inclusion of intra-coded macroblocks (MBs) within predictively-coded frames [5].

Nevertheless, it is still necessary to protect the whole of the bitstream (without privileging the A and B-partitions) against the risk of packet loss through channel error. Application-layer forward error correction of datapartitioned NALUs is achieved by means of rateless channel codes. In particular, Raptor codes [6], which are a systematicvariety of rateless code, are Maximum Separable Distance codes (as are Reed-Solomon (RS) codes) but unlike RScodes also have linear decode complexity. By means of a single ARQ triggered retransmission, the proposed scheme exploits rateless coding's main feature, the ability to generate redundant data on the fly.

WiMAX provides broadband wireless access independently of the need for a pre-existing cellular system, is not dependent on hardware authentication, can deliver data in a cost-effective way at 3–4 times the rate of 3G cellular systems, and is currently deployed, rather than in the development stage. Its main technological weakness may be that it uses Orthogonal Frequency Division Multiple Access (OFDMA) for both uplink and the downlink transmission rather than OFDMA for the downlink and Single Carrier-Frequency Division Multiple Access (SC-FDMA), which confers power-saving advantages upon Long Term Evolution (LTE) [7]. IPTV is one form of multimedia service that is an attractive application of WiMAX but previous proposed solutions have been mainly at the physical layer (PHY) [8] rather than the application layer. The inclusion of ARQ may preclude a broadcast IPTV, but video-on-demand is a useful value-added service in addition to the basic broadcast

service.

Data partitioning in this paper works *without* the need to apply privileged or unequal error protection to the A- and Bpartitions. This is achieved by setting the variable-bit-rate video's quantization parameter (QP) in such a way that lower-priority texture data, which can be compensated for more easily at the decoder, occupies a larger proportion of a video frame's compressed data. Consequently, when partition data are packetized in a WiMAX MAC Service Data Unit (MSDU) within a MAC Protocol Data Unit (MPDU), the longer packet is more likely to suffer error than MSDUs bearing data from other partitions. However, the decoder can apply motion copy error concealment to reconstruct missing C-partition data by means of the motion vectors still available in the A-partition.

We have found through simulation of our scheme that there are a number of trade-offs present. As ARQ triggered retransmissions of redundant data increase the delay increases before a frame's compressed data can be reconstructed. Reduction of the number of retransmissions by increasing the percentage of redundant rateless data can reduce this delay but this may be at a cost of reduced video quality, as there is a net decrease in the redundant data sent. It is also important to consider the effect of a scheme upon the number of packet drops at the base station's buffer, as these packets cannot be reconstructed using the rateless code. Another important point to notice is that that streaming is sensitive to the size of the WiMAX Time Division Duplex (TDD) frame, as a smaller TDD frames causes fewer packets to be removed from the base station (BS) buffer, causing more drops at the BS until the next queue service time.

Therefore, the contribution of this paper is an IPTV video-on-demand streaming scheme for WiMAX employing data-partitioning and rateless coding in a new and effective mix. A higher percentage of Intra-macroblocks for decoder refresh than is normal improves the delivered video quality.
The paper analyses the balance between latency and video quality within a WiMAX context. The following Section gives the context of the proposed scheme. Section III details the simulation model used to evaluate the proposed scheme in Section IV, while Section V makes some concluding remarks and indicates further research.

II. CONTEXT

A. Data-partitioning

The H.264/AVC codec conceptually separates the Video Coding Layer (VCL) from the NAL. The VCL specifies the core compression features, while the NAL supports delivery over various types of network. This network-friendliness feature of the standard facilitates easier packetization and improved video delivery. In a communication channel the quality of service is affected by the two parameters of bandwidth and the probability of error. Therefore, as well as video compression efficiency, which is provided for through the VCL layer, adaptation to communication channels should be carefully considered. The concept of the NAL, together with the error resilience features in H.264/AVC, allows communication over a variety of different channels.

The NAL facilitates the delivery of the H.264 VCL data to the underlying transport layers such as RTP/IP, H.32X and MPEG-2 systems. Each NAL unit could be considered as a packet that contains an integer number of bytes including a header and a payload. The header specifies the NALU type and the payload contains the related data. Table I is a summarized list of different NALU types. NALUs 6 to 12 are non-VCL units containing additional information such as parameter sets and supplemental information.

In H.264/AVC, when data-partitioning is enabled, every slice is divided into three separate partitions and each partition is located in either of type 2 to type-4 NALUs, as listed in Table I. NALU of type 2, also known as partition A, comprises the most important information of the compressed video bit-stream of P- and B-pictures, including the MB addresses, motion vectors and essential headers. If any MBs in these pictures are intra-coded, their Discrete Cosine Transform (DCT) coefficients are packed into the type-3 NALU, also known as partition B. Type 4 NAL, also known as partition C, carries the DCT coefficients of the motion-compensated inter-picture coded MBs. It is worth noting that as in I-slices all MBs are encoded, then type 5 NALUs are very long. On the other hand A and B partitions of data-partitioned P- and B-slices are much smaller but their C-type partition can be very long.

TABLE I. NAL UNIT TYPES

NAL unit type	Class	Content of NALU
0	-	Unspecified
1	VCL	Coded slice
2	VCL	Coded slice partition A
3	VCL	Coded slice partition B
4	VCL	Coded slice partition C
5	VCL	Coded slice of an IDR picture
6-12	Non-VCL	Suppl. info., Parameter sets, etc.
13-23	-	Reserved
24-31	-	Unspecified

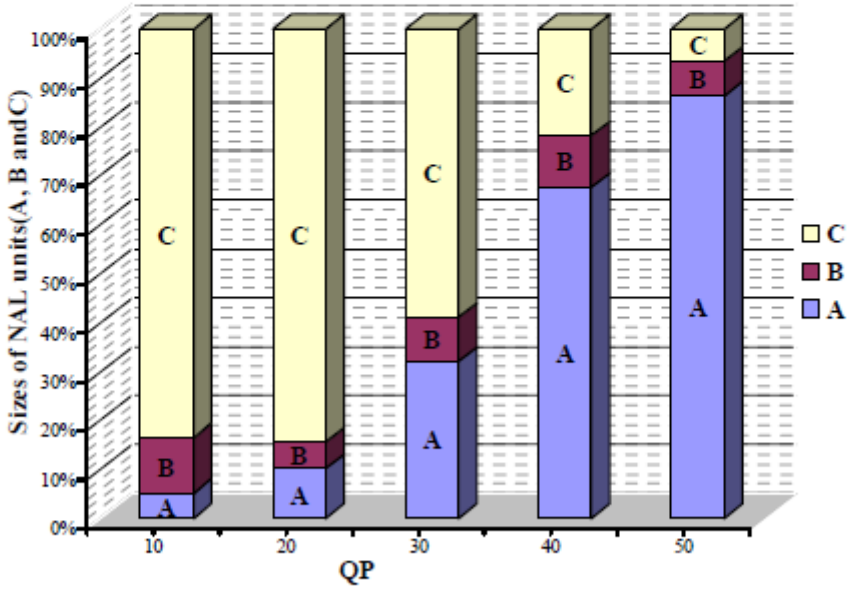

Figure 1. Relative sizes of data partitions according to quantization parameter (QP) for Paris video clip

Fig. 1 is a comparison between the relative sizes of the partitions according to QP for the tested video clip. In H.264/AVC the QP range is from 0 to 51, with a low QP representing high quality. The Paris sequence is a studio scene with two head and shoulders images of presenters.

The background is of high spatial complexity. Paris was encoded at Common Intermediate Format (CIF) (352× 288 pixel/frame), with a Group of Picture (GOP) structure of IPPP….. at 30 frame/s (Hz). Experiments not shown indicate that including B-Pictures, with a GOP structure of IPBP (sending order) … and intra-refresh rate of 15, did not noticeably disturb this pattern. The same can be said if the Stefan clip with much more motion is included. We reserve future work to elaboration of a simple 'rule of thumb' to determine a QP that best benefits the data-partitioning scheme. This will depend on the proportion of intra-coded MBs, which has the effect of changing the relative size of the B-partition's contribution.

The relatively small size of the A- and B-partitions is a potential advantage at high QPs but this comes at a cost of a high bitrate. Conversely, at the low quality end of the QP range, (say) QP = 40, if no protection is afforded to Apartition NALs, then they become relatively vulnerable to packet loss by virtue of their relatively increased length.

B. Rateless coding

A fixed-rate (n, k) Reed-Solomon (RS) channel code over an alphabet of size $q = 2^L$ has the property that if *any* k out of the n symbols transmitted are received successfully then the original k symbols can be decoded. However, for RS coding not only must n, k, and q be small but also the computational complexity of the decoder is of order $n(n - k)\log_2 n$. The error rate must also be estimated in advance.

In contrast, the class of Fountain codes [9] allows a continual stream of additional symbols to be generated in the event that the original symbols could not be decoded. It is the ability to easily generate new symbols that makes Fountain codes rateless. Decoding will succeed with small probability of failure if any of k $(1 + \varepsilon)$ symbols are successfully received. In its simplest form, the symbols are combined in an exclusive OR (XOR) operation according to the order specified by a random low density generator matrix and in this case, the probability of decoder failure is $\partial = 2^{-k\varepsilon}$, which for large k approaches the Shannon limit. The random sequence must be known to the receiver but this is easily achieved through knowledge of the sequence seed.

Luby Transform (LT) codes [10] reduce the complexity of decoding a simple Fountain code (which is of order k^3) by means of an iterative decoding procedure, provided that the column entries of the generator matrix are selected from a robust Soliton distribution. In the LT generator matrix case, the expected number of degree one combinations (no XORing of symbols) is $S = c \log_e(k/\partial)\sqrt{k}$, for small constant c. Setting $\varepsilon = 2\log_e(S/\partial)$ S ensures that by sending $k(1 + \varepsilon)$ symbols these are decoded with probability $(1 - \partial)$ and decoding complexity of order $k \log_e k$.

If packets are pre-encoded with an inner code, a weakened LT transform can be applied to the symbols and their redundant symbols. The advantage of this Raptor code [6] is a decoding complexity that is linear in k. A systematic Raptor code is arrived at [6] by first applying the inverse of the inner code to the first k symbols before the outer precoding step.

III. SIMULATION MODEL

A. Rateless coding evaluation

In order to model Raptor coding, we employed the following statistical model [11]:

$$P_f(m,k) = 1 \quad \text{if } m < k,$$
$$= 0.85 \times 0.567^{m-k} \text{ if } m \geq k \qquad (1)$$

where $P_f(m,k)$ is the failure probability of the code with k source symbols if m symbols have been received. The authors of [11] remark and show that for $k > 200$ the model almost perfectly models the performance of the code. In the experiments reported in this paper, the percentage redundancy for the Raptor code was set by default to 10% similarly to the usage in [12] for video streaming. However, the redundancy level was then varied to 5% and 15%, as a check on whether the setting was appropriate. The symbol size was set to bytes within a packet. Clearly, if instead 200 packets are accumulated before the rateless decoder can be applied (or at least equation (1) is relevant) there is a penalty in start-up delay for the video streaming and a cost in providing sufficient buffering at the mobile stations.

A corrupt packet can be detected by the Cyclic Redundancy Check (CRC) that is an optional part of the MPDU (WiMAX packet), refer to Fig. 2. Though this CRC also applies to the 4-byte MAC header, it does indicate the likelihood that a packet's payload is corrupt. Then, through measurement of channel conditions, an estimate of the number of symbols successfully received is made, giving a value m'. This implies from (1) that if less than k symbols (bytes) in the payload are successfully

received then $k-m'+1$ redundant bytes can be sent to reduce the risk of failure to below 50%. Clearly, it is possible to improve the failure risk by simply including more bytes. However, in this paper we
confine repeat transmissions of redundant bytes to a minimal amount, as we have found that video quality remains good. Future work will explore the effect on video quality of increasing the amount of redundant data retransmitted.

To reduce latency, the number of retransmissions, after an ARQ over the uplink, was limited to one. The effect of this decision can be judged by the results in Section IV. Fig. 3 shows how ARQ triggered retransmissions work. In the Figure, packet X is corrupted to such an extent that it cannot be reconstructed. Therefore, in packet X+1 some extra redundant data is included up to the level that its failure is no longer certain. If the extra redundant data is insufficient to reconstruct the original packet, the packet is simply dropped. Otherwise, of course, it is passed to the H.264/AVC decoder.

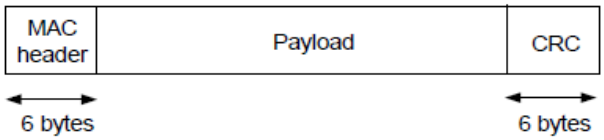

Figure 2. General format of a MAC PDU with optional CRC.

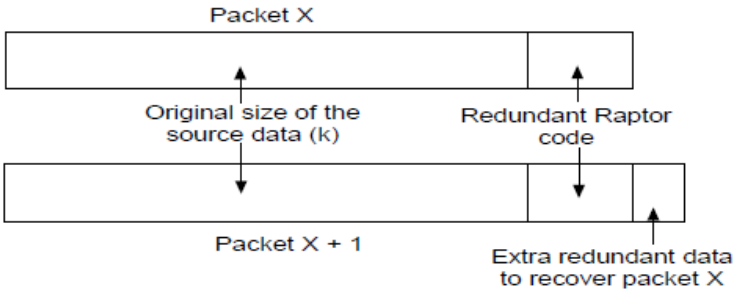

Figure 3. Division of payload data in a packet (MPDU) between source data, original redundant data and piggybacked data for a previous errored packet.

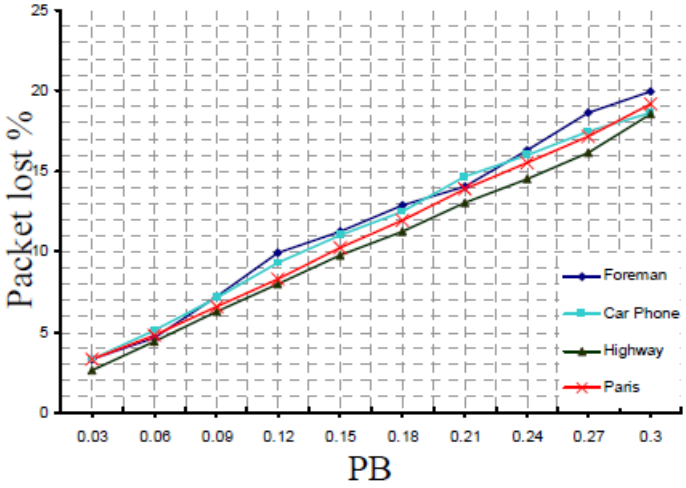

Figure 4. The relationship between Gilbert-Elliott bad probability (PB) and packet loss rate for different video sequences.

The WiMAX standard already specifies [13] that a subscriber station (SS) should provide channel measurements that can form a basis for channel quality estimates. These are either Received Signal Strength Indicators or may be Carrier-to-Noise-and Interference Ratio measurements made over modulated carrier preambles.

B. Channel model

To establish the behaviour of rateless coding under WiMAX the well-known ns-2 simulator augmented with a module from the Change Gung University, Taiwan that has proved an effective way of modelling IEEE 802.16e's behaviour. We also introduced a two-state Gilbert-Elliott channel model [14] in the physical layer of the simulation to simulate the channel model for WiMAX. The PGG (probability of being in a good state) was set to 0.95, PBB (probability of being in a bad state) = 0.96, PG (probability of losses in a bad state) = 0.02 and PB (probability of losses in a bad state) = 0.165 for the Gilbert-Elliott parameters.

As an illustration of the effect, Fig. 4, the PB was increased by 0.03 until 0.3. Four different 30 Hz video datapartitioning traces with CIF spatial resolution were utilized. The packet loss percentage was calculated to find the relationship between the lost packets and PB. From Fig. 4, it is apparent that as much as the PB is increased the packet loss percentage is increased, as might be expected. However, because of the different coding complexities and types of complexity (spatial and temporal) the effect on video quality will be somewhat different.

C. WiMAX configuration

The physical layer (PHY) settings selected for WiMAX simulation are given in Table II. The antenna is modelled for comparison purposes as a half-wavelength dipole. The TDD frame length was varied in experiments, because it has an important effect on the service rate at the BS. Video was transmitted over the downlink with UDP transport. In order

TABLE II. IEEE 802.16 PARAMETER SETTINGS

Parameter	*Value*
PHY	OFDM
Frequency band	5 GHz
Bandwidth capacity	10 MHz
Duplexing mode	TDD
Frame length	8 to 20 ms
Max. packet length	1024 B
Raw data rate	10.67 Mbps
IFFT size	1024
Modulation	16-QAM 1/2
Guard band ratio	1/8
DL/UL ratio	3:1
Channel model	Gilbert-Elliott
MS transmit power	245 mW
BS transmit power	20 W
Approx. range to SS	1 km
Antenna type	Omni-directional
Antenna gains	0 dBD
MS antenna height	1.2 m
BS antenna height	30 m

OFDMA = Orthogonal Frequency Division Multiple Access, QAM = Quadrature Amplitude Modulation, TDD = Time Division Duplex

to introduce sources of traffic congestion, an always available FTP source was introduced with TCP transport to the SS. Likewise a CBR source with packet size of 1000 B and inter-packet gap of 0.03 s was downloaded to the SS. While the CBR and FTP occupy the non-rtPS (non-real-time polling service) queue, rather than the rtPS queue, they still contribute to packet drops in the rtPS queue for the video, if the 50 packet rtPS buffer is already full or nearly full, while the nrtPS queue is being serviced. We are aware that this congestion configuration is just one of many and future work should investigate this dimension of the problem.

D. Video configuration

The Paris sequence, mentioned in Section II.A was employed for the WiMAX downlink tests. Paris with 1064 CIF frames was Variable Bit Rate (VBR) encoded at c. 15 Hz. The slower frame rate is more typical of mobile device displays. As a GOP structure of IPPP.... was employed it is necessary to protect against error propagation in the event of inter-coded P-frame slices being lost. To ensure higher quality video, 25% intra-coded macroblocks (randomly placed) to act as anchor points in the event of slice loss. The advantage of the GOP configuration is that it allows H.264/AVC's baseline profile to operate with reduced codec complexity due to the absence of Bi-predictive B-frames. At the decoder motion copy error concealment was set, allowing the motion vectors contained in A-partition packets to indicate suitable replacement macroblocks within the last correctly received slice. The JM 14.2 version of the H.264 codec software was employed with the Evalvid environment used to reconstruct sequences according to reported packet loss from the simulator.

IV. EVALUATION

Two types of erroneous packets were considered: 1) packet drops at the BS sender buffer and 2) corrupted packets that were received but affected by Gilbert-Elliott channel noise to the extent that they could not be immediately reconstructed without an ARQ triggered retransmission. Notice that if the retransmission of additional redundant data still fails to allow the packet to be reconstructed then the packet is simply dropped. The Raptor code equation (1) was applied to decide if a packet could be recovered, given the number of bytes that were declared to be in error.

Tests first checked whether partitioning a frame into three was responsible for the gain from data-partitioning or whether the gain actually arose from the segregation of the information when using data-partitioning. The comparison was made across QP values and across WiMAX TDD frame sizes. Therefore, in the non-data-partitioning sliced tests, an encoded frame was geometrically divided into three equal sized horizontal slices (simple slicing). For these tests the Raptor code percentage was set to 10%.

Comparing Tables III and IV, it is apparent that geometric slicing has an advantage when it comes to the number of dropped packets when transmitting very high quality video (QP = 10). This is because of the much larger C-partition packets when data-partioning is used at this QP. Therefore, if data-partioning is used the impact of packet drops must be considered or guarded against. Otherwise, data-partitioning is preferable in terms of the final objective video quality. The small fluctuations in the number of corrupted packets between the two schemes makes little difference to the objective video quality for QPs higher than 10. One can conclude that more C-partition packets than A- and Bpartition packets are corrupted, leading to the superior quality of the data-partioned solution, even though no special protection is given to A- and B-partition packets. Independent analysis not reported herein for reasons of space confirmed that more C- than A- and B-partition packets were dropped.

Examining the variation in WiMAX TDD frame size, the larger frame size brings a reduction in dropped packets at the BS buffer, as more data are removed from the buffer at each visit of the scheduler. Though commercial settings are difficult to establish it could be that a low TDD frame size as small as 5 ms could be common. Though in these tests the differential effect of TDD frame size was not strong enough to impact the final PSNR figures, a scenario could easily arise in which there was an impact.

Though other tests were performed to check the performance of data-partitioned packetization without Raptor code, the high loss rate of A-partition packets prevented the decoder reconstructing the video. The packet mean end-to-end delay was also found. This was compared with the mean latencies in

delivering a packet's data to the decoder buffer taking into account retransmissions triggered by a (single) ARQ. Considering the end-to-end delay for the data-partitioning scheme in Table V, this tends to reduce with smaller packet size and higher QP. There is also a reduction in latency with longer TDD frame size. The first effect is the result of on average longer transmission times, while the latter effect can be explained by reduced queueing times. There is a considerable overall time penalty in introducing even single ARQ generated retransmissions. In simple slicing there are no larger packets to weigh the delay averages upwards. However, it is unclear why there is little delay variation dependency on QP and, hence, slice size and why queuing appears to increase with larger TDD frame size. For the sliced schemes, end-to-end delay and data latency are generally below 30 ms and 50 ms respectively, except for the highest quality video transported with data-partitioning. Therefore, for these schemes buffers at the SS can be small.

TABLE V. MEAN LATENCIES FOR THE TWO SCHEMES COMPARED.

	Data partitioning packet end-to-end delay (s)		
QP	8 ms TDD	10 ms TDD	20 ms TDD
10	0.072	0.064	0.053
15	0.019	0.025	0.029
20	0.012	0.019	0.022
25	0.009	0.016	0.020
QP	Data partitioning data latency (s)		
10	0.195	0.094	0.083
15	0.050	0.055	0.059
20	0.042	0.049	0.052
25	0.039	0.046	0.050
	Simple slicing packet end-to-end delay (s)		
QP	8 ms TDD	10 ms TDD	20 ms TDD
10	0.008	0.015	0.019
15	0.008	0.015	0.019
20	0.008	0.015	0.019
25	0.008	0.015	0.019
QP	Simple slicing data latency (s)		
10	0.038	0.045	0.049
15	0.038	0.045	0.048
20	0.038	0.045	0.048
25	0.038	0.045	0.049

TABLE VI. MEAN PERFORMANCE WITH 5% REDUNDANT DATA

	Dropped packets (%)		
QP	8 ms TDD	10 ms TDD	20 ms TDD
10	14.1	2.8	0.3
15	0	0	0
20	0	0	0
25	0	0	0
	Corrupted packets (%)		
QP	8 ms TDD	10 ms TDD	20 ms TDD
10	4.59	4.57	4.68
15	4.70	4.79	4.54
20	4.46	4.54	4.77
25	4.58	4.64	4.65
	PSNR (dB)		
QP	8 ms TDD	10 ms TDD	20 ms TDD
10	35.11	42.49	47.06
15	46.97	42.98	46.97
20	42.53	42.53	42.98
25	39.02	39.02	39.30
	Packet end-to-end delay (s)		
QP	8 ms TDD	10 ms TDD	20 ms TDD
10	0.059	0.057	0.050
15	0.019	0.025	0.028
20	0.012	0.019	0.022
25	0.009	0.016	0.020
	Data latency (s)		
QP	8 ms TDD	10 ms TDD	20 ms TDD
10	0.723	0.253	0.198
15	0.082	0.083	0.086
20	0.072	0.076	0.080
25	0.074	0.077	0.080

A. Changing the redundancy level

The effect of changing the percentage of redundant code in the original packets was examined (refer to Table VI) by decreasing the rateless overhead to 5% in the datapartitioning scheme. Paradoxically, the overall video quality (PSNR) is improved by including less redundant data even though the percentage of corrupted packets increases considerably. This is explained by the inadequacy of 5% data redundancy in reconstructing approaching 50% of the packets. As a consequence the number of ARQ triggered retransmissions increases considerable, despite a small reduction in the end-to-end packet delay (because of the smaller packet sizes with less redundant data).

V. CONCLUSIONS

This paper proposed that data-partitioning when employed with Raptor rateless coding can result in good quality video for a video-on-demand IPTV. However, the transfer of streaming scheme to a

particular broadband wireless technology is a multi-dimensional problem, as there are many trade-offs, which the paper illustrated. Therefore, our results are preliminary and are dependent on a variety of settings such as buffer size and intra-MB proportion. The ratio of redundant data sent originally and that sent after an ARQ triggered retransmission deserves further investigation as part of an adaptive scheme.

REFERENCES

1] IEEE, 802.16e-2005, Part 16: Air Interface for Fixed and Mobile Broadband Wireless Access Systems, 2005.

[2] Intel Inc., "H.264 & IPTV over DSL", Whitepaper, 12 pages, 2004.

[3] P. Ferré, et al., "Robust video transmission over wireless LANs," IEEE Trans. Vehicular Technol., vol. 57, no. 4, pp. 2596-2602, 2008

[4] S. Wenger, "H.264/AVC over IP," IEEE Trans. Circuits Syst. Video Technol. , vol. 13, no. 7, pp. 645-655, 2003.

[5] M. N. Hannuksela, Y.-K. Wang, and M. Gabbouj, "Random access using isolated areas," IEEE Int'l Conf. on Image Processong, pp. 841- 844, 2003 .

[6] A. Shokorallahi, "Raptor codes," IEEE Trans. Information Theory, vol. 52, no. 6, pp. 2551-2567, 2006.

[7] K. Ekstrom et al., "Technical solutions for the 3G Long-Term Evolution," IEEE Commun. Mag., vol. 44, no. 3, pp. 38-45, 2006.

[8] J. She, F. Hou, P.-H. Ho, and L.-L. Xie, "IPTV over WiMAX: Key success factors, challenges, and solutions," IEEE Commun. Mag. , vol. 45, no. 8, pp. 87-93, 2007.

[9] D. J. C. MacKay, "Fountain codes," IEE Proc.: Communications, vol. 152, no. 6, pp. 1062–1068, 2005.

[10] M. Luby, "LT codes," in 34rd Annual IEEE Symp. on Foundations of Computer Science, pp. 271–280, Nov. 2002.

[11] M. Luby, T. Gasiba, T. Stockhammer, and M. Watson, "Reliable multimedia download delivery in cellular broadcast networks," IEEE Trans. Broadcasting, vol. 53, no. 1, pp. 235-246, 2007.

[12] S. Ahmad, R. Hamzaoui, M. Al-Akaidi, "Robust live unicast video streaming with rateless codes", in Int'l PacketVideo Workshop, Nov. 2007.

[13] L. Nuaymi, WiMAX: Technology for Broadband Wireless Access, J. Wiley & Sons Ltd, Chichester, UK, 2007.

[14] G. Haßlinger and O. Hohlfeld, "The Gilbert-Elliott model for packet loss in real time services on the Internet," in 14th GI/ITG Conf. on Measurement, Modelling, and Evaluation of Computer and Commun. Systs. , pp. 269-283, 2008.